International Journal of Advanced Technology in Engineering and Science www.ijates.com
Volume No.03, Issue No. 04, April 2015 ISSN (online): 2348 - 7550

SYNTHESIS OF ZNO QUANTUM DOT BY SELF ASSEMBLY METHOD AND ZNO NANOROD BY HYDROTHERMAL METHOD

Abdulla M.Suhail[1], Wasan R. Saleh[2], Omar A. Ibrahim[3], Rawa K.Ibrahim[4]

[1]Dept.of Optical Techniques, Dijlah University College, Iraq

[2,3]Physics Department, College of Science, University of Baghdad, Iraq

[4]Advanced Materials Reaserch Center, Ministry of Science and Technology, Iraq

ABSTRACT

In this work, ZnO quantum dots (Q.dots) and nanorods were prepared. ZnO quantum dots were prepared by self-assembly method of zinc acetate solution with KOH solution, while ZnO nanorods were prepared by hydrothermal method of zinc nitrate hexahydrate Zn $(NO_3)_2.6H_2O$ with hexamethy lenetetramin (HMT) $C_6H_{12}N_4$. The optical , structural and spectroscopic properties of the product quantum dot were studied. The results show the dependence of the optical properties on the crystal dimension and the formation of the trap states in the energy band gap. The deep levels emission was studied for n-ZnO and p-ZnO. The preparation ZnO nanorods show semiconductor behavior of p-type, which is a difficult process by doping because native defects.

Keyword: Zno, Quantum Dots, Nanorods, Deep Levels, Self-Assembly

I. INTRODUCTION

Semiconductor nanoparticles have recently attracted significant attention for their role in fundamental studies and technical applications [1]. Zinc oxide (ZnO) is a II–VI semiconductor material with a wide band gap of about (3.37 eV) together with a high exciton binding energy of (60 meV) both at room temperature rendering ZnO to receive global attention especially in connection with the emerging nanotechnology paces toward functionality ZnO has a very high ionization potential (~8eV) and electron affinity (~4.7eV) that partially explains the ease to obtain n-doping [2]. Zinc oxide is a versatile material that has achievable applications in photo-catalysts, varistors, sensors, piezoelectric transducers, solar cells, transparent electrodes, electroluminescent devices and ultraviolet laser diodes. It has stimulated extensive research and many nanometer photoelectron components [3-7]. Self-assembly of colloidal particles is low cost and self-organization growth behavior enabling the growth of ZnO nanostructures on any substrate material regardless of lattice matching issues [2]. Self-assembly of colloidal particles into larger aggregates is not principally new but was used to prepared quantum dot by Claudia Pacholski et al [8]. ZnO quantum dots have superior optical properties of the bulk crystals owing to quantum confinement effects. Understanding the electronic and optical characterizations in ZnO quantum dot is important from both a fundamental science and a proposed photonic application point of view. Absorption (UV) and photoluminescence (PL) spectra were widely used to investigate the edge emission from ZnO quantum dot; however, direct observation of the band gap variation upon particle

size from PL is relatively rare. In this work, growth of ZnO quantum dot and the dependence of the optical properties on the crystal dimension and the formation of the trap states in the energy band gap were studied.

More applications for trap states are in optoelectronics device and white light generation [9]. The native defect in ZnO it was resulted to intrinsic deep level emission in band gap [10].

Nanorods are solid nanostructures morphologically similar to nanowires but with aspect ratios of approximately 3-5. They are formed from a variety of materials including metals, semiconducting oxides, diamonds, and organic materials [11]. ZnO nanorod is a semiconductor; its optical band gap can be tuned by changing the morphology, composition, size and etc. because the electron affinity for ZnO is (~4.7eV) that partially explains the ZnO must be electron injected. Therefore, the growth was difficult of p-type ZnO with good electrical and optical properties. Because of the intrinsic (native deep defects) properties of ZnO such as the high self-compensation of donor defects, the limited acceptors as well as the deeper acceptor level, it is difficult to achieve p-type ZnO by impurity doping. Although many scientists from different research groups have attempted various doping methods, a stable high grade p-type ZnO is still hard to obtain [12-14]. In p-type doped ZnO, oxygen vacancies (V_O) assumes a two charge state and hence provides a potential source of compensation in p-type ZnO. Oxygen vacancy (V_O) deep level defects, can contribute to the unintentional n-type conductivity of ZnO when present as complexes, but not as isolated native point defects [10]. Finally, the position of the extrinsic hydrogen energy level is also depicted, as this plays an important role in the n-type conductivity of ZnO. Hydrogen mentions due to its important role as a donor for the electrons (n-type ZnO). Unlike other semiconductors where hydrogen can be positive or negative, hydrogen in ZnO is always positive (H+), *i.e.*, it acts as a donor and possesses low ionization energy [15, 16].

Recent years, ZnO nanorods have been intensely used to fabricate nano-scale electronic devices, including field effect transistor, ultraviolet photo detector, Schottky diode, and ultra-bright light-emitting diode (LED). Various methods have been developed to fabricate the single crystalline, wurtzite ZnO nanorods [17].

Achieving control over ZnO nanorod morphology is a challenging task. Various synthesis methods have been investigated and used in ZnO nanorods fabrication, reported in [18-22]. These growth techniques are complicated and growth temperatures used are high at about 800 C. The hydrothermal method [23] has attracted considerable attention because of its unique advantages. It is a simple, low temperature (60–100 C), high yield and more controllable process. It is believed that synthesis without catalysts and templates is a better technique for large-scale production of well-dispersed nanorods [2]. In the present work, the dependence of ZnO nanorod morphology on precursor compositions and solution growth conditions was investigated.

1.1 Luminescent Centers in ZnO

The room temperature PL spectrum of ZnO nanostructure with diameters larger than 20 nm is similar to the PL spectra of bulk ZnO. This is normally characterized by near band-edge (NBE) ultra-violet (UV) emission and at least one broad band emission due to deep levels, called the broad band extending, from just above (400-750) nm, *i.e.*, the whole visible spectrum. The broadness of the band results from the fact that it represents a superposition of many different deep levels emitting at the same time. Although no consensus exists on the origin of the broad deep band emission, the broad nature of the emission suggests the possibility that it is a combination of many emissions. The deep levels of ZnO are divided into extrinsic and intrinsic deep levels. The possible intrinsic ‘native’ deep levels in ZnO are oxygen vacancy (V_O), zinc vacancy (V_{Zn}), oxygen interstitial

(O_i), zinc interstitial (Zn_i), oxygen anti-site (O_{Zn}), and zinc anti-site (Zn_O). This is in addition to native defect clusters, which are usually formed by the combination of two point defects or one point defect and one extrinsic element, these levels called deep–level-emission (DLE) [10]. The different energy levels of the different deep-level defects reported by different groups as shown in fig. (1)

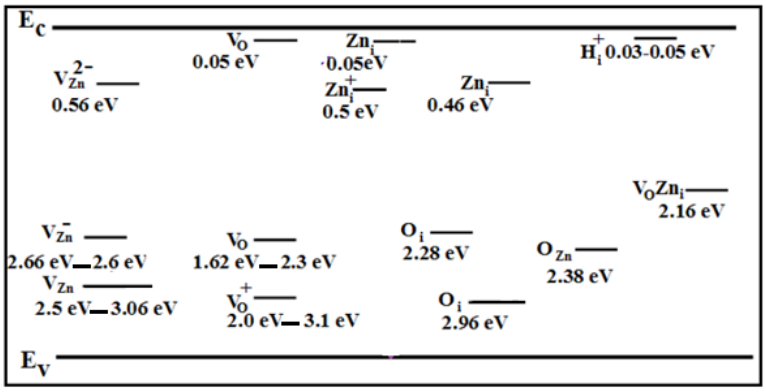

Fig. (1): Energy Levels of the Different Deep Level Defects in ZnO [10]

In figure (1), the + and – symbols represent charged deep levels. Three shallow levels are also shown, due to neutral oxygen vacancies, positively charged extrinsic hydrogen, and neutral zinc interstitials. In addition, the position of the deep level due to V_OZn_i clusters is indicated.

Most of these native defects introduce deep levels at different positions in the band gap, and hence a rather large number of luminescence lines with different energies can be observed. This explains why all of the visible colors have been experimentally observed in different ZnO samples. The common bands observed in ZnO are green, yellow, and red luminescence DLE bands. Table (1) summarized all transition for the native defect states.

Table (1): Some recently reported lines emitted from ZnO and the proposed associated deep level defect causing the emission. The conduction and valence bands are abbreviated in the usual way as C.B. and V.B., respectively.

Emission color (nm)	Proposed deep level transition
Violet	Zni to V.B.
Blue	Zni to VZn or C.B. to VZn
Green	C.B. to VO, or to VZn, or C.B. to O_{Zn}
Yellow	C.B. to Oi or Zni to Oi
Red	Lattice disorder along the c-axis (*i.e.* due to Zni) or Zn_i to O_i

These DLE can invest in the generation more lights colors and white light generation by electroluminescence and photoluminescence device [9].

II. EXPERIMENTAL WORK

2.1 Preparation of ZnO Quantum Dot

Quantum dots of ZnO were prepared as a colloidal by self–assembly method. All materials which used to synthesis process were supplied from Fluka Company. 0.01M of zinc acetate dehydrate ($Zn(CH_3COO)_2 .2H_2O$) solution was prepared by dissolved 1.25 mmol of zinc acetate in 125 ml of methanol under vigorous stirring at about 60^oC subsequently. A 0.03M of potassium hydroxide (KOH) solution was prepared by dissolved 2mmol of KOH in 65 ml of methanol. KOH solution was added drop wise to zinc acetate solution and the reaction mixture was stirred for 2h at 60^oC [8]. In order to synthesis quantum dots more regular, the pH of mixture used

to be (8.5). The transparency color of zinc acetate solution will start to change to the white after added the KOH solution. After 1h, the color will change to transparent white which indicate the starting of synthesis ZnO Q.dots. After 2h the color will turn to opaque white which means that the amounts of formed ZnO Q.dots start increasing. The formed Q.dots can be separated by using the centrifuge and stored in ethanol. The sample was annealed in at 300^0C in vacuum. The fact that upon proper post-growth annealing, the hydroxyl group (OH) can desorb [10] and hence modifies the emission from that of the as-grown ZnO nanostructure and lessening the lattice strain [24].

2.2 Preparation of ZnO Nanorods

The growth of the ZnO nanorods were carried out by deposited the ZnO Q.dots solution on substrate by spin coating technique. This process was applied three times were a rational coverage is expected. A chemical path deposition at 60^oC was used for the covered substrates by, immersed in a solution contain 0.15 M of zinc nitrate hexahydrate $Zn(NO_3)_2.6H_2O$ mixed with 0.1M of hexamethylenetetramine $O_6H_{12}N_4$ (HMT) in volume ratio 1:1. The substrates were pulled and put it in the aqueous solution and kept in oven for 2h at 60^oC. The growth samples were soaked in distilled-water under ultrasonic agitation to remove the un-reacted salts, and then left to dry at room temperature [2].

III. RESULTS AND DISCUSSION

The crystal graphic orientation of ZnO Q.dots and ZnO nanorods was analyzed by using a Shimadzu 6000 x-ray diffractometer using Cu kα radiation of wavelength 1.5406 A. XRD pattern was recorded at a scanning rate of $0.08333^o s^{-1}$ in the 2θ range from $30^o - 70^o$ as given in fig.s (2 and 3). These Figures shows that the prepared ZnO Q.dot and ZnO nanorods have poly crystalline structure. It is clear that the formed Q.dots have wurtzite structure. The XRD pattern consist of many diffraction peaks and strong orientation peak at $2\theta = 36.28^o$ which is belong to (101) diffraction line. Furthermore no impurities were found in the patterns. Also the diffraction peaks are intensive and very sharp. Thus high purity wurtzite ZnO nanocrystals could be obtained by this synthesis process.

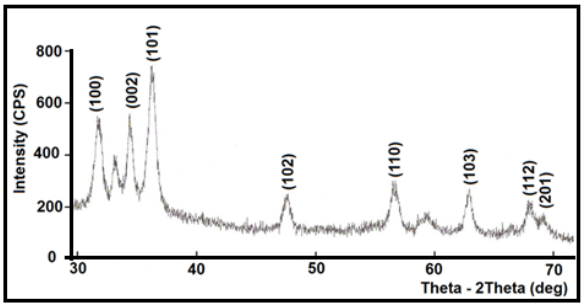

Fig. (2): X-ray Diffraction Pattern of ZnO Q.dot

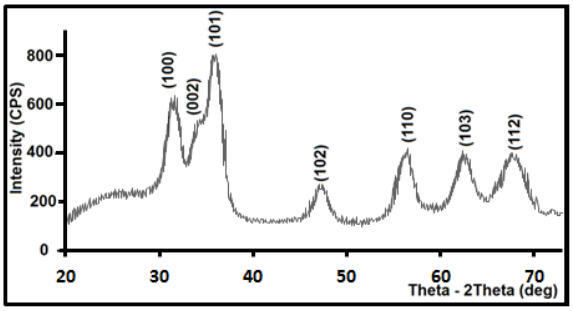

Fig. (3): X-ray Diffraction Pattern of ZnO Nanorods

The formed Q.dot size after annelid the sample at 300^0C is calculated by Scherrer's equation (eq1) and found to be 9 nm

$$d = \frac{0.9\lambda}{\beta\cos\theta} \qquad (1)$$

where: d is the quantum dot size, λ is the wavelength for X-ray source ,β is the full width at half maximum FWHM and θ is the diffraction angle[24].

The structure morphology for the samples was analyzed by using VEGA3 TESCAN, high vacuum mode SE from TESCAN ORSAY HOLDING, while the morphology surface analysis was carried out employing on CSPM AA3000 PFM supplied by Angstrom Company Fig. (4) show images of SEM at magnification of 50 Kx for the prepared ZnO Q.dots and ZnO nanorod respectively. Fig. (4a) reveals that the shape of formed Q.dots is approximately spherical, while the inset image shows aggregation of Q.dots in the range of 200 nm. Fig. (4b) given a prove to the formation of nanorods in the range of (~30 nm width and 300 nm length).

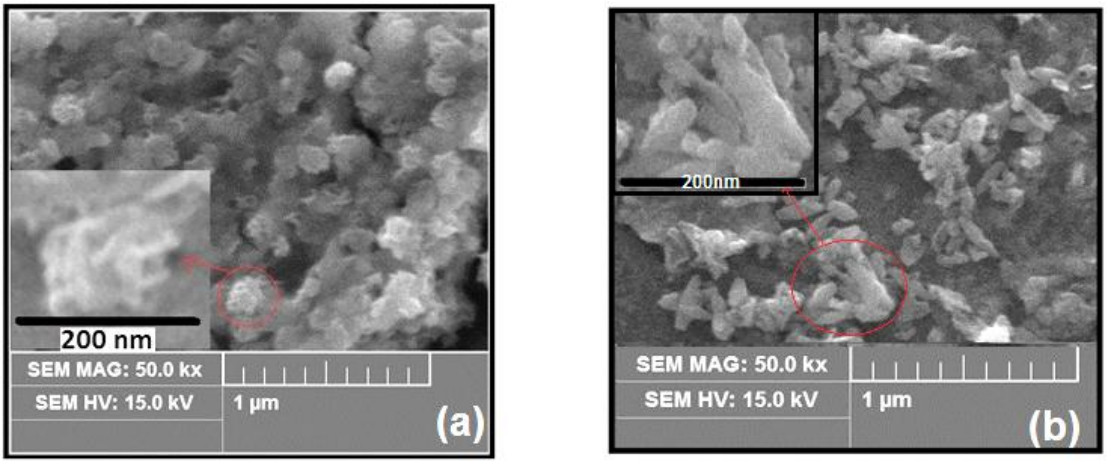

Fig. (4): SEM Images of (a) ZnO Q.dot and (b) ZnO nanorods

To remove the aggregation, dissolved the ZnO Q.dots in chloroform and deposited on the glass substrate

Fig. (5) shows the SEM images of formed ZnO quantum dot after removed the aggregation. The figure reveals that the shape of formed Q.dots is approximately spherical, the inset image shows that the grain size of Q.dots are in the range of 20 nm, while the crystal size was about 9 nm according to the XRD test.

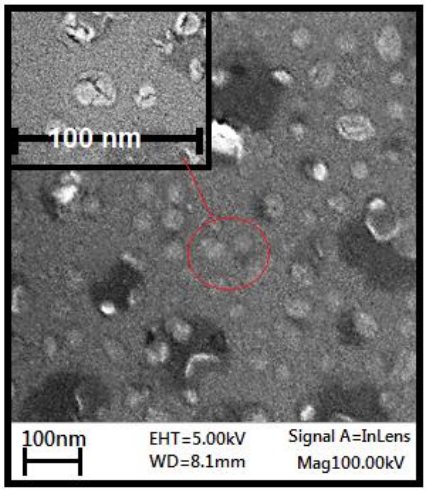

Fig. (5): SEM Images of ZnO Q.Dots after Remove the Aggregation and Inset Different between Grain Size and Crystal Size

Fig. (6) shows two dimensional AFM images of the surface topography of ZnO Q.dots and ZnO nanorods prepared at 60^{o}C. The images show the uniformity distribution for Q.dots and nanorods and appear the spherical shape of dots. The surface roughness average is very small which indicates that the samples have smooth

surface. Surface topography parameters and average grain size which estimated from the granularity copulation distribution are tabulated in Table (2).

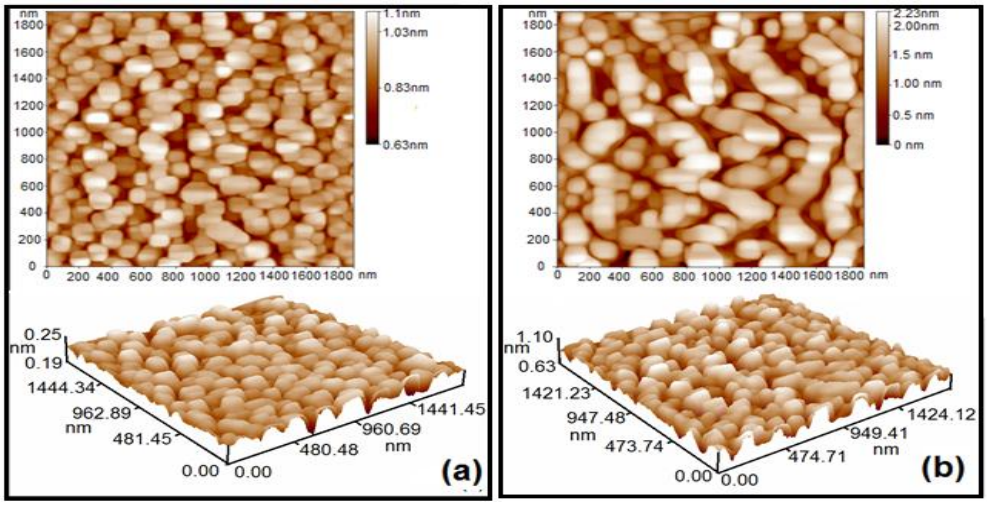

Fig. (6): AFM Two Dimensional Images of (a) ZnO Q.dot and (b) ZnO Nanorods

Table (2) : Surface topography parameters and grain sizes of ZnO Q.dots and nanorods

Sample parameters	Q.dots (nm)	Nanorods (nm)
Surface roughness average (Sa)	0.0671	0.3821
Root mean square roughness (Sq)	0.0845	0.461
Ten point height (Sz)	0.299	1.46
Average grain size (GS)	60	30(for width)

The optical properties of the ZnO Q.dots and ZnO nanorods were investigated after deposited on a quartz substrate. The absorbance of the samples was measured by LABOMED.INC spectra UV/Vis double beam scanning, covering range from (190 – 1100) nm. The absorbance spectrum as a function of the wavelength in the range (190 – 690) nm is shown in fig. (7). It is clear that the film has very high absorbance in the UV region and decreases exponentially with the increasing of wavelength, which indicates that ZnO Q.dots have high response in the UV region.

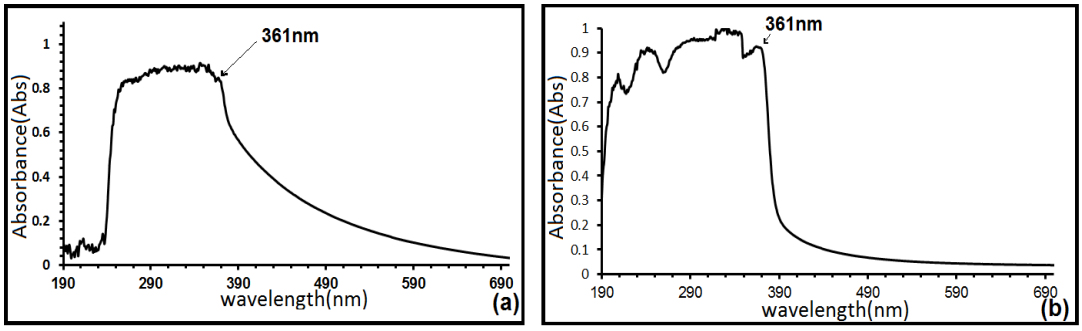

Fig. (7): The Absorbance Spectrum of: (a) ZnO Q.dots and (b) ZnO Nanorods

The figure shows a prominent exciton band at 361nm corresponds be the ZnO nanostructures. This absorption peak is blue shifted as compared to the bulk exciton absorption of ZnO (368 nm), which is due to the size effect of the nanostructures. The absorption spectrum of the Q.dots implies that there exist more defect energy levels (trap stats or surface stats), due to the specific experimental conditions.

The absorption spectrum for ZnO nanorods (fig. 7b) shows that the sample becomes transparent to the visible light due to nanorods growth.

The energy band gap from the absorbance spectrum was calculated by Tauc relation [25], according to the relation between the photo energy ($h\upsilon$) and $(\alpha h\upsilon)^2$, equation (2).

$$\alpha h\upsilon = B\,(h\upsilon - Eg)^r \qquad (2)$$

Where B is constant, h is the Plank's constant, υ is the photon frequency, α is the absorption coefficient, Eg is the optical energy gap, and r is a parameter that has different values (1/2,1,3/2,2) according to the type of transition.

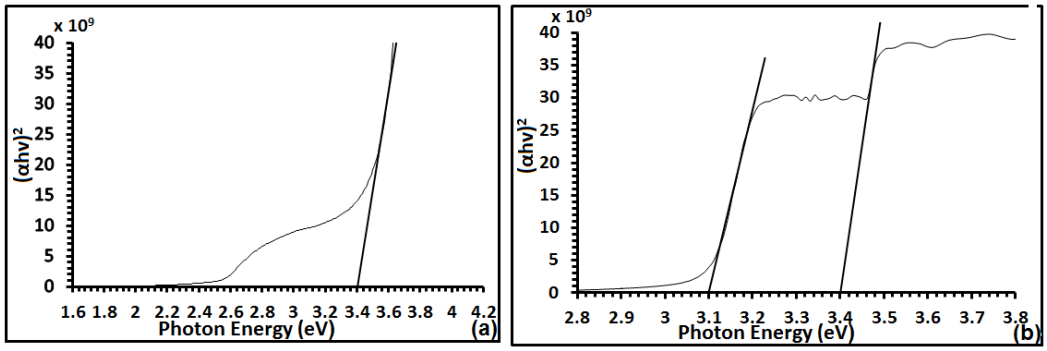

Fig. (8): $(\alpha h\upsilon)^2$ vs. Photon Energy for: (a) ZnO Q.dots and (b) ZnO Nanorods

In fig. (8) the extrapolation of the liner part of $(\alpha h\upsilon)^2$ vs. photon energy ($h\upsilon$) gives energy gap of about 3.41eV for both ZnO Q.dots and nanorods. This value of energy gap was quite comparable with value the.

It is observed from fig. (8a) there are two absorption edges. The first edge is related to the band-to-band transition which is equal to 3.41 eV. The second edge equal to 3.1eV is related to native deep defect levels for the nanorods which attributed to the transition from V_{Zn} to Zn_i or V.B to Zn_i.

Quantum dot size (diameter) was calculated from Brus equation (3) [26].

$$E_{g.q.dot} = E_{g.bulk} + \frac{2\hbar^2\pi^2}{e\,d^2\,m_0}\left(\frac{1}{m_e}+\frac{1}{m_h}\right) - \frac{1.8e}{2\pi\varepsilon\varepsilon_0 d} \qquad (3)$$

where $Eg_{Q.dot}$ is the quantum dot band gap, Eg_{bulk} is the bulk band gap, m_e is the electron effective mass (=0.26 for ZnO), m_h is the hole effective mass (=0.59 for ZnO), e is the charge electron, d is the diameter of quantum dot, m_0 is the free electron mass, ε_o is the permittivity of free space, and ε is the relative permittivity. By applying equation (3), the Q.dots size is around (7.3 and 8.8) nm correspond to the energy gap for (photoluminescence spectrum was equal 3.43eV and absorption spectrum was equal 3.41eV) respectively.

Eq (3) was used also to calculate the confinement for electron in crystal. Since in nanorods there is no confinement for the electron in the length of the rod, so that equation (3) cannot used to calculate the dimensions of nanorods.

The PL spectrum was measured using VARIAN fluorescence spectrophotometer, supplied by Eclipse Company with the spectrum range from (190-1100) nm. PL studies provide information for different energy deep states available between valance bands and conduction bands, which responsible for the irradiative recombination. These states are called trap states, which is caused the emission peaks.

The PL spectrum of ZnO Q.dots and ZnO nanorods excited by 300 nm wavelength is shown in fig. (9).

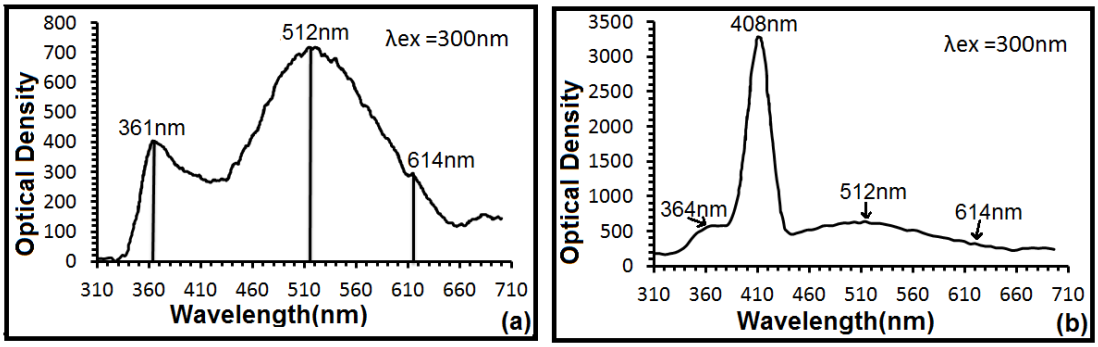

Fig. (9): The PL Spectrum of: (a) ZnO Q.dots and (b) ZnO Nanorods.

In fig. (9), the first peak centered at 361 nm which is refers to band–to–band transition (meat the energy gap) .The energy gap for the first peak from PL spectrum for ZnO Q.dots was calculated using equation (4) and found to be 3.43eV, while the energy gap from absorbance spectrum is 3.41 eV. This is consider normal difference.

$$E_g\,(eV) = \frac{1240}{\lambda(nm)} \qquad (4)$$

The origin of trap states is came from the intrinsic deep levels this is means native deep levels, as explain in fig. (11). Fig. (9a) shows three peaks, the first peak centered at 361 nm (violet) which is refers to band – to –band transition (meat the energy gap) and the remaining peaks belonging to the trap stats. Show fig. (10)

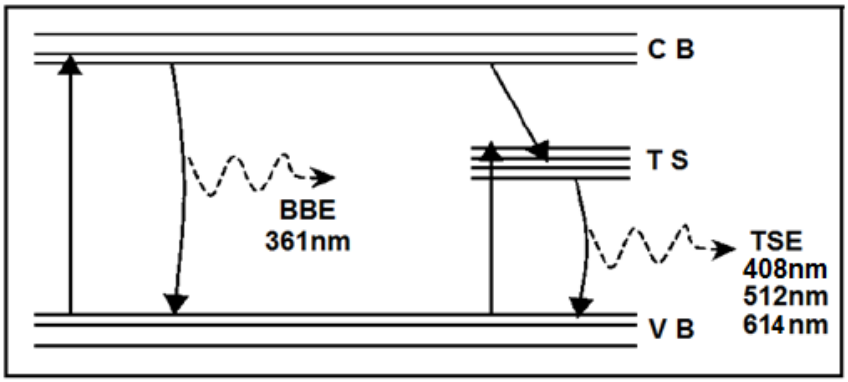

Fig. (10): Photon Excited Emission Spectra of ZnO q. Dot and ZnO Nanorods [27]. where: BBE is the Band to Band Emission, TS is the Trap Stats and TES is the Trap State Emission

The second peak centered at 512 nm (green), this peak is broad according to the inner transition in the same time which includes the yellow, green and little from orange region. These colors resulted through native deep levels; yellow reign C.B to O_i or Zn_i to O_i and green region C.B to V_O or to V_{Zn} or C.B to both V_O and V_{Zn}. The third peak centered at 614 nm (red) is due to lattice disorder along the c-axis (due to Zn_i) or excited Zn_i states.

Form fig. (9b), it is clear that the PL spectrum of ZnO nanorods is similar for that of ZnO Q.dots in the position of peaks centered at (361,512 and 614) nm. This is because the nature of formation the nanorods which is have the similar energy of Q.dots. In the same figure, fourth peak was appeared at 408nm (violet) which is belong to the transition through native deep levels transition between C.B to V_{Zn} or Zn_i to V_{Zn}. These transitions described by the schematic in fig. (11). The figure shows large number of luminescence lines with different energies. This explains why all of the visible colors have been experimentally observed in ZnO nanostructure samples.

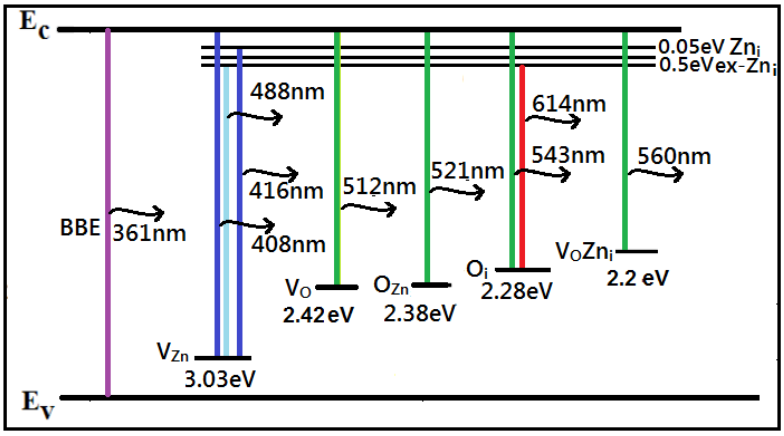

Fig. (11): Energy Levels of the Different Deep Level Defects in ZnO Q.dot and ZnO Nanorods

ZnO Q.dots film was electrically characterized using Hall Effect measurement. The film of 550 nm thickness shows semiconductor behavior of n-type conductivity. The conductivity and resistivity values were $4.13X10^{-6}$ $(\Omega\ cm)^{-1}$ and $2.42X10^{5}$ $(\Omega\ cm)$ respectively, while the mobility was $2.53X10^{1}(cm^2/V\ sec)$.

The process of synthesis ZnO nanorods leads to have ZnO nanorods shows semiconductor behavior of p-type conductivity. This convert in the behavior devolves to change in shape. V_{Zn} states are derived from the broken bonds of the oxygen's nearest four neighbors. These states are partially filled and can accommodate an electron, causing V_{Zn} to act as an acceptor. (That V_{Zn} levels are deep acceptors). This means p-type was formed and this is clearly appear in PL spectrum from the luminescence of V_{Zn}.

The conductivity and resistivity values for ZnO nanorods were $2\ X10^{-5}$ $(\Omega\ cm)^{-1}$ and $5X10^{4}$ $(\Omega\ cm)$ respectively, while the mobility was $1.2X10^{1}(cm^2/V\ sec)$

IV. CONCLUSIONS

Simple and low cost method was used to synthesis ZnO Q.dots and nanorods successfully. This method given good optical properties because of appearance of the defect states which was important in generating of white light by photoluminescence and electroluminescence. Our method leads to obtained p-type ZnO nanorods by growth nanorods without doping.

REFERENCES

[1]. A.B. Djurišić and Y.H. Leung,Optical Properties of ZnO Nanostructures , Small,2(8-9), (2006) 944–961.

[2]. A. Zainelabdin, S. Zaman, G. Amin, O. Nur,and M. Willander, Stable White Light Electroluminescence from Highly Flexible Polymer/ZnO Nanorods Hybrid Heterojunction Grown at 50C, Nanoscale Res Lett ,5, (2010) ,1442–1448

[3]. S. C. Minne, S. R. Manalis, and C. F. Quate, Parallel atomic force microscopy using cantilevers with integrated piezoresistive sensors and integrated piezoelectric actuators, Appl. Phys. Lett.,67(26), (1995), 3918-3920.

[4]. Baxter, J.B.; Aydil, E.S.,Nanowire based dye sensitized solar cells, Applied Physics Letters , 86(5), (2005) ,3114-3117.

[5]. C. A. Wolden, J. B. Baxter, T. M. Barnes, and E. S. Aydil, Infrared detection of hydrogen generated free carriers in polycrystalline ZnO thin films, Journal of Applied Physics,97(4), (2005), 3522-3524.

[6]. R. Ko¨nenkamp, R.C. Word, C. Schlegel ,Vertical nanowire light emitting diode, Appl. Phys. Lett.,85(24) , (2004), 6004-6006.

[7]. Z.K. Tang, G.K.L. Wong, P. Yu, M. Kawasaki, A. Ohtomo, H. Koinuma, Y. Segawa,Room-temperature Ultraviolet Laser Emission from Self-assembled ZnO Microcrystalline Thin Films, Appl. Phys. Lett. 72, (1998), 3270-3272.

[8]. C. Pacholski, A. Kornowski, and H. Weller,Self-Assembly of ZnO: From Nanodots to Nanorods, Angew. Chem. Int. Ed., 41(7), (2002), 1188-1191.

[9]. A.M. Suhail1, M.J. Khalifa, N.M. Saeed1, and Omar. A. Ibrahim, "White light generation from CdS nanoparticles illuminated by UV-LED", Eur. Phys. J. Appl. Phys., 49,(2010) ,30601.

[10]. M. Willander , O. Nur, J. R. Sadaf, M. I. Qadir, S. Zaman, A. Zainelabdin, N. Bano and I. Hussain,Luminescence from Zinc Oxide Nanostructures and Polymers and their Hybrid Devices, Materials, 3, (2010), 2643-2667.

[11]. A.-Sistos, J.G. Rosas, R. Esparza, R. Pérez,BN Nanorod Production Using Mechanical Alloying, Advances in Technology of Materials and Materials Processing,7(2), (2005), 175-180.

[12]. Kim H, Cepler A, Osofsky MS, Auyeung RCY, Pique A Fabrication of Zr-N codoped p-type ZnO thin films by pulsed laser deposition, Appl. Phys. Lett.,90(20), (2007), 2035081-3.

[13]. Sun MH, Zhang QF,Wu JL,Electrical and electroluminescence properties of As-doped p-type ZnO nanorods arrays, J. phys. D Appl. phys., 40(12), (2007), 3798-3802.

[14]. Ohta H, Mizoguchi H, Hirano M, Narushima S, Kamiya T, Hosono H.,Fabrication and characterization of heteroepitaxial p-n junction diode composed of wide-gap oxide semiconductors p-$ZnRh_2O_4$/n-ZnO, Appl. Phys. Lett.,82(5),(2003), 823–825.

[15]. Chris G. Van de Walle,Hydrogen as a Cause of Doping in Zinc Oxide, Physical review letters, 85(5),(2000), 1012-1015.

[16]. Y. He, J.-An Wang, X.-Ban Chen, W.-Fei Zhang, X.-Yu Zeng and Q.-Wen Gu,Blue electroluminescence nanodevice prototype based on vertical ZnO nanowire/polymer film on silicon substrate, J. Nanopart Res.,4(12), (2010), 169–176.

[17]. G.-Chul Yi, C. Wang and W. I. Park, ZnO nanorods: synthesis characterization and applications, Semiconductor Science and Technology, 20(4), (2005), S22–S34.

[18]. W. I. Park , Gyu-Chul Yi , J.W. Kim and S.-M. Park, Schottky nanocontacts on ZnO nanorod arrays, APPLIED PHYSICS LETTERS, 82(24),(2003).

[19]. N. I. Rusli, M. Tanikawa, M. R. Mahmood, K. Yasui and A. Hashim,Growth of High-Density Zinc Oxide Nanorods on Porous Silicon by Thermal Evaporation, Materials,5(28),(2012), 17-32.

[20]. K.C.-Yong Oh, H.-bong ; R., Hyukhyun ; Y. J. Lee and W.-Jae ,ZnO nanorod growth by plasma-enhanced vapor phase transport with different growth durations, Journal of Vacuum Science & Technology A: Vacuum, Surfaces and Films, 32(5), (2014).

[21]. S.-Sik Park, J.-Moo Lee, S.-Jin Kim and S.-Woo Kim ,Catalyst – Free synthesis of ZnO Nanorods on Metal substrates by using thermal chemical vapor deposition, Journal of the Korean Physical Society,53(1), (2008), 183-187.

[22]. O. Akhavan , M. Mehrabian, K. Mirabbaszadeh and R. Azimirad ,Hydrothermal synthesis of ZnO nanorod arrays for photocatalytic inactivation of bacteria, Journal of Physics D: Applied Physics,42(22), (2009), 5305-5309.

[23]. K.H. Tam, A.B. Djurisic , C.M.N. Chan, Y.Y. Xi, C.W. Tse, Y.H. Leung, W.K. Chan, F.C.C. Leung and D.W.T. Au, Antibacterial activity of ZnO nanorods prepared by a hydrothermal method, Thin Solid Films, 516(18), (2008), 6167–6174.

[24]. C.Suryanarayana and M.G.Norton,X-ray Diffraction A practical Approach, Plenum press, New York, 207-221, (1998).

[25]. Tauc, J.,Optical properties and electronic structure of amorphous Ge and Si, Materials Research Bulletin, 3(1), (1968), 37–46.

[26]. K.-Feng Lin, H.-Ming Cheng, H.-Cheng Hsu, L.-Jiaun Lin, W.-Feng Hsieh, Band gap variation of size-controlled ZnO quantum dots, Chemical Physics Letters .409 , (2005), 208–211.

[27]. James W. M. Chon and Min Gu.,Three-photon excited band edge and trap emission of CdS semiconductor nanocrystals, Appl. Phys. Lett., 84(22), (2004), 4472-4474.